Temperature-Humidity Dependent Wind Effects on Physiological Heat Strain of Moderately Exercising Individuals Reproduced by the Universal Thermal Climate Index UTCI

Peter Bröde * and Bernhard Kampmann

Posted Date: 3 May 2023

doi: 10.20944/preprints202305.0152.v1

Keywords: heat stress; air temperature; humidity; wind; heat wave; electrical fan; index

Article

Temperature-Humidity Dependent Wind Effects on Physiological Heat Strain of Moderately Exercising Individuals Reproduced by the Universal Thermal Climate Index UTCI

Peter Bröde [1,*] and Bernhard Kampmann [2]

[1] Leibniz Research Centre for Working Environment and Human Factors at TU Dortmund (IfADo), Ardeystrasse 67, D-44139 Dortmund, Germany; broede@ifado.de
[2] School of Mechanical Engineering and Safety Engineering, Department of Occupational Health Science, University of Wuppertal, Germany; kampmann@uni-wuppertal.de
* Correspondence: broede@ifado.de; Tel.: +49 231 1084 225

Simple Summary: With climate change exacerbating heat extremes, there is a growing need for sustainable measures reducing physiological heat strain. However, public health policies have issued warnings against the use of electric fans and ventilators at ambient temperatures exceeding typical skin temperatures of 35 °C. Aiming to extend previous findings for sedentary persons to moderately exercising individuals, we analyzed heart rates, sweat rates, core and skin temperatures recorded in 198 climatic chamber experiments with 3h-exposures to treadmill work under widely varying heat stress conditions. Our findings suggest mitigating wind effects at temperatures above 35 °C when humidity was elevated. Moreover, the close agreement of the observed effects with the corresponding wind effects predicted by the Universal Thermal Climate Index *UTCI* demonstrates the potential of *UTCI* for evaluating sustainable strategies of heat stress mitigation for moderately exercising individuals.

Abstract: Increasing wind speed alleviates physiological heat strain, however, health policies have advised against using ventilators or fans under heat wave conditions with air temperatures above the typical skin temperature of 35 °C. Recent research, mostly with sedentary participants, suggests mitigating effects of wind at even higher temperatures depending on the humidity level. Our study aimed at exploring and quantifying, whether such results are transferable to moderate exercise levels, and whether the Universal Thermal Climate Index *UTCI* reproduces those effects. We measured heart rates, core and skin temperatures and sweat rates in 198 laboratory experiments completed by five young, semi-nude, heat-acclimated, moderately exercising males walking the treadmill with 4 km/h on the level for three hours under widely varying temperature-humidity combinations and two wind conditions. We quantified the cooling effect of increasing wind speed from 0.3 to 2 m/s by fitting generalized additive models predicting the physiological heat stress responses depending on ambient temperature, humidity and wind speed. We then compared the observed wind effects to the assessment performed by *UTCI*. Increasing wind speed lowered physiological heat strain for air temperatures below 35 °C, but also for higher temperatures with humidity levels above 2 kPa water vapour pressure concerning heart rate and core temperature, and 3 kPa concerning skin temperature and sweat rate, respectively. *UTCI* assessment of wind effects correlated positively with the observed changes in physiological responses, showing the closest agreement (r=0.9) for skin temperature and sweat rate, where wind is known for elevating the relevant convective and evaporative heat transfer. These results demonstrate the potential of *UTCI* for adequately assessing sustainable strategies for heat stress mitigation involving fans or ventilators depending on temperature and humidity for moderately exercising individuals.

Keywords: heat stress; index; air temperature; humidity; wind; heat wave; electrical fan

 doi:10.20944/preprints202305.0152.v1

1. Introduction

1.1. Sustainable heat stress mitigation by wind

Climate change accelerating with fossil energy use will exacerbate heat extremes, which will provoke physiological heat strain in terms of increased heart rates, core and skin temperatures, and sweat rates imposing health risks [1,2] and potentially affecting human performance and productivity [3,4]. Elevating air movements by outdoor wind or ventilators is a cost-effective and sustainable measure for mitigating physiological heat strain [5–7]. However, policies and public health authorities have advised against electric fan use under heat wave conditions with air temperatures above the typical skin temperature of 35 °C, because convective cooling will then turn to convective heating of the body [8–10]. On the other hand, the well-known enhancement of sweat evaporation with increased wind speed [11–13] challenged these postulations and advocated for an evidence-based approach [14]. Recent studies, mostly with sedentary participants [15,16], demonstrated cooling effects of ventilation due to enhanced sweat evaporation with even higher temperatures at elevated humidity levels.

Comparative studies involving experimental heat exposures are usually restricted to a few well-defined climatic conditions [15]. Thus, for separating beneficial cooling from detrimental heating wind effects over a grid of temperature-humidity conditions in heat wave scenarios, several studies applied biophysical modelling based on human heat balance calculation [17–20]. Interestingly, qualitatively similar threshold curves based on modelling the naturally aspirated wet-bulb temperature had been developed one century ago [21]. These curves indicated wind cooling at elevated humidity levels, but additional heat load in hot-arid climates, as flagged by the term 'poison wind' (*simoom*) for potentially fatal outdoor conditions in Southwest Asian desert regions [21]. Notably, the simulations of heat wave scenarios only considered resting conditions concerning metabolic rates of about 1 MET (1 MET=58.2 W/m^2), whereas physical load at workplaces and many home and outdoor activities are associated with metabolic rates higher than 2 MET [22,23].

Concerning physiological heat strain under moderate exercise levels, the recorded heart rates, core and skin temperatures, and sweat rates in Figure 1 from an extensive database of climate chamber experiments [24,25] exemplify the aforementioned findings for an acclimated young male walking 4 km/h on a treadmill corresponding to 2.3 MET metabolic rate. While increasing air velocity from 0.3 to 2 m/s lowered physiological heat strain in a hot-humid climate with air temperature exceeding skin temperature (Fig. 1a), increased wind amplified heat strain under hot-dry conditions (Fig. 1b). Figure A1 in the Appendix A includes a supporting example from another participant. In both cases, the transient overshooting of sweat rate with low wind (v_a = 0.3 m/s) under warm-humid conditions (Fig. 1a) may be explained by hidromeiosis [26], which did not occur when increasing wind speed to v_a = 2.0 m/s enhanced sweat evaporation [27].

A recent study with exercising participants [28] examined how wind speed at various temperature-humidity combinations affected physical work capacity, defined by the workload related to metabolic rate, which the participants could tolerate with heart rate clamped at 130 beats per minute (bpm). Coupling their experimental data with heat balance calculations, they showed beneficial wind effects for air temperatures up to 44 °C with relative humidity exceeding 50%, but detrimental wind effects for higher temperatures. Similar findings had been reported concerning the shift of the critical, i.e. tolerable humidity level by wind in hot environments [29]. Another study [30] showed beneficial wind effects for sports activities at specific conditions with 37 °C air temperature and 50% relative humidity.

However, there is a lack of data from controlled laboratory experiments specifying wind effects on physiological heat strain in terms of heart rates, core and skin temperatures, and sweat rates while covering a wide grid of air temperature-humidity combinations.

Preprints (www.preprints.org) | NOT PEER-REVIEWED | Posted: 3 May 2023 doi:10.20944/preprints202305.0152.v1

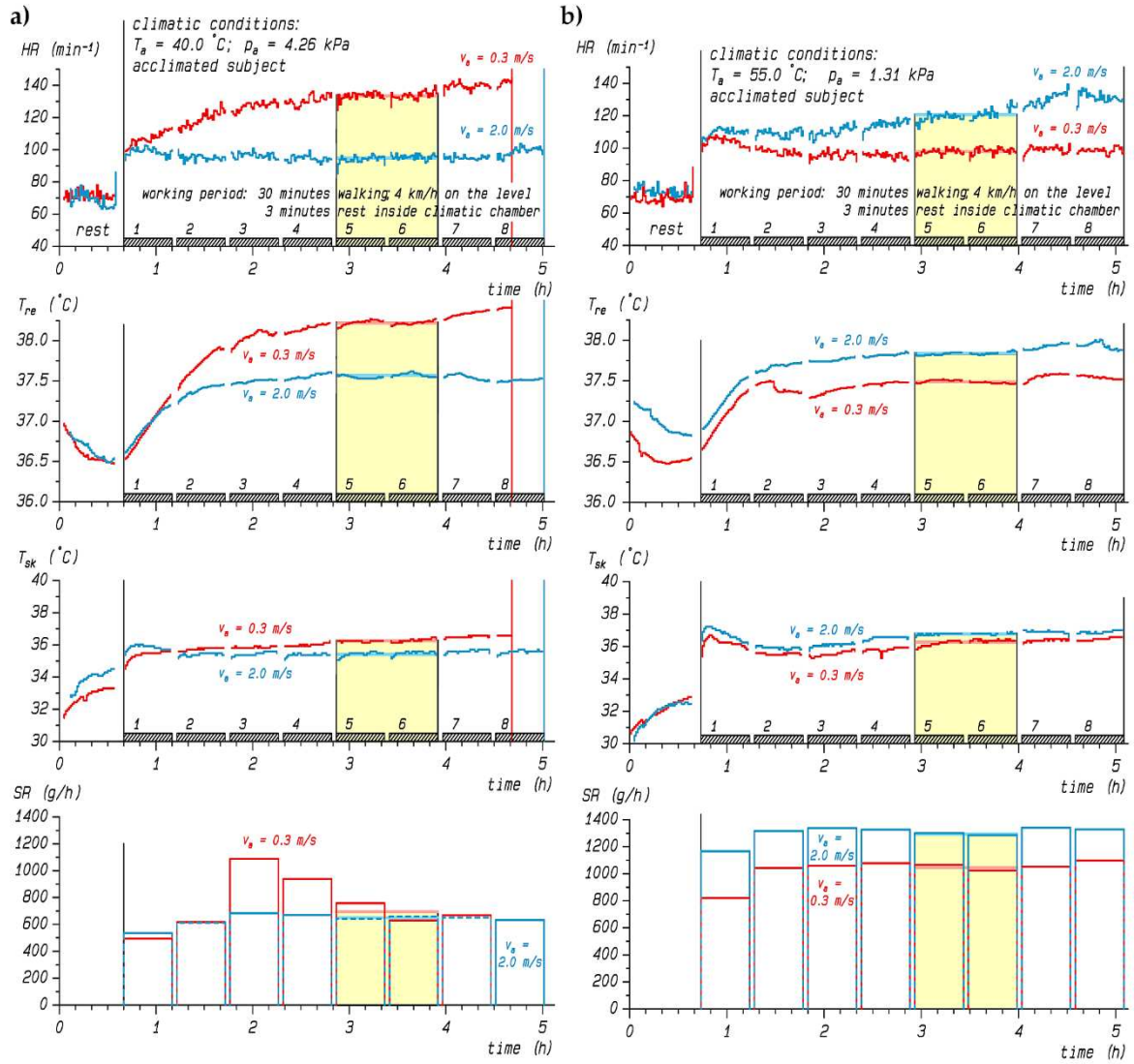

Figure 1. Time course of heart rate (*HR*), rectal (T_{re}) and mean skin temperature (T_{sk}), and sweat rate (*SR*) of an acclimated participant during experiments in a hot-humid climate (**a**) or in a hot-dry climate (**b**) under both reference (v_a = 0.3 m/s) and high air velocity (v_a = 2 m/s) conditions. The yellow shaded area marks the time interval with averaged values used for analyses. Note that the reference wind trial in (a) was prematurely aborted in the 8th working period.

In addition to data requirements, there seems to be a need for improving the thermo-physiological modelling beyond the heat balance approach, as recent findings suggest that the simple models will underestimate physiological heat strain under electrical fan use, e.g. for the vulnerable elderly population [31].

When looking for advanced, but easy-to-use modelling approaches, the Universal Thermal Climate Index *UTCI* [32] developed for moderately active persons (2.3 MET) constitutes a noteworthy alternative. The index was constructed from the dynamic physiological thermal strain simulated by the advanced *UTCI*-Fiala model of human thermoregulation [33] coupled with an adaptive clothing model [34]. *UTCI* allows for the assessment of the thermal environment covering the range from extreme cold to extreme heat stress conditions. The model was extensively validated [35], and showed good agreement with thermal environment standards and experimental data in occupational settings [36–38]. Though *UTCI* relies on sophisticated models, the operational procedure [39] provides algorithms making it easily applicable, e.g. for assessing the wind cooling potential of actual and future urban scenarios in relation to wind direction [40]. Concerning the effects on physical work capacity, *UTCI* outperformed any other considered thermal index in capturing not only the effects of

Preprints (www.preprints.org) | NOT PEER-REVIEWED | Posted: 3 May 2023 doi:10.20944/preprints202305.0152.v1

wind over a wide grid of temperature-humidity conditions [28], but also in combination with heat radiation [41].

1.2. UTCI sensitivity to wind

Following meteorological conventions, *UTCI* calculations rely on air velocity 10 m above ground ($v_{a,10m}$). For conversion to any other measurement height, e.g. 1 m for person level, the operational procedure [39] provides a logarithmic formula shown in Eq. 1, indicating that air velocity at person level ($v_{a,1m}$) is computed as the 10 m value ($v_{a,10m}$) divided by 1.5, in accordance with international standards [42].

$$v_{a,1m} = v_{a,10m} \times log(1/0.01) / log(10/0.01) = v_{a,10m} / 1.5 \quad (1)$$

As the *UTCI* person is assumed to move on the level with 4 km/h, corresponding to a walking speed v_w = 1.1 m/s, this is taken into account by calculating the resulting or relative air velocity at person level ($v_{ar,1m}$) according to Eq. 2. Here, α denotes the angle between the directions of walking and wind, assigned to zero for indicating the same direction. As *UTCI* does not assume a specific angle, $v_{ar,1m}$ is calculated by integrating Eq. 2 over all α between zero and 2π [34,43].

$$v_{ar,1m} = \sqrt{(v_w - v_{a,1m} \times \cos\alpha)^2 + (v_{a,1m} \times \sin\alpha)^2} \quad (2)$$

Figure 2 presents the resulting $v_{ar,1m}$ used by *UTCI* for calculating the convective and evaporative heat loss [33]. Notably, reducing wind speed below $v_{a,10m}$ = 0.5 m/s ($v_{a,1m}$ = 0.3 m/s) will hardly impact $v_{ar,1m}$, which is limited by v_w, while $v_{ar,1m}$ will approach $v_{a,1m}$ for $v_{a,10m}$ above 3 m/s.

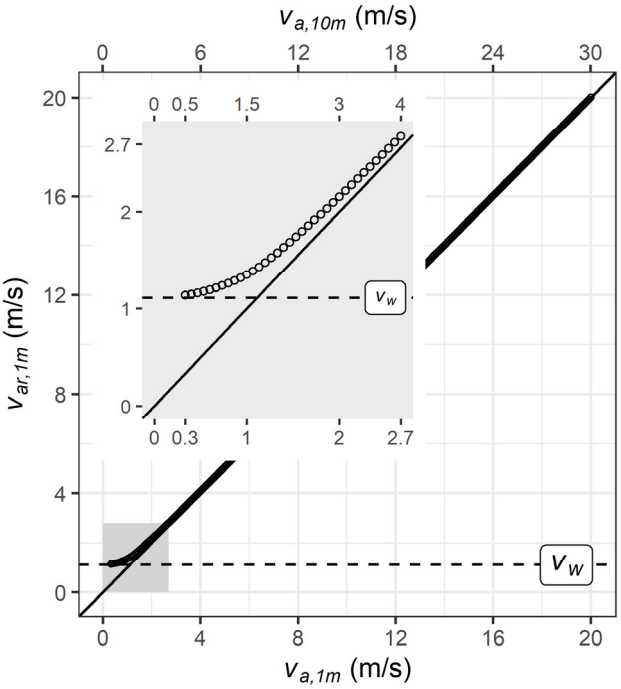

Figure 2. Relative wind speed at person level ($v_{ar,1m}$) when moving with the *UTCI* reference walking speed (v_w) of 4 km/h corresponding to 1.1 m/s, in relation to wind speed measured at person level ($v_{a,1m}$) and at 10 m above ground ($v_{a,10m}$). The insert provides a detailed view of the grey-shaded region for $v_{a,10m} \leq 4$ m/s. Figures include solid lines of identity, and horizontal dashed lines indicating walking speed (v_w).

1.3. Study objectives

Based on a comprehensive physiological heat strain database [24], this study aimed at exploring and quantifying whether reports on beneficial wind effects with air temperature exceeding skin

Preprints (www.preprints.org) | NOT PEER-REVIEWED | Posted: 3 May 2023 doi:10.20944/preprints202305.0152.v1

temperature under humid conditions for sedentary individuals are transferable to moderate exercise levels, and whether the Universal Thermal Climate Index *UTCI* reproduces these effects.

2. Materials and Methods

2.1. Experimental data

We compiled a database of climate chamber experiments conducted previously at IfADo [24,44] according to the ethical principles of the Declaration of Helsinki after approval by IfADo's local Ethics Committee.

We searched our database for series of heat stress experiments with participants exercising on a treadmill under both reference (***RefWind***, with air velocity v_a = 0.3 m/s) and high wind (***HiWind***, v_a = 2 m/s) conditions. Inclusion criteria were a minimum number of 15 experiments per series with comparable workload and clothing. We retrieved 198 trials organized in 10 series, which originated from five acclimated semi-nude (basic clothing insulation I_{cl} = 0.1 clo, 1 clo = 0.155 $\underline{K}\cdot\underline{m^2}\cdot\underline{W^{-1}}$) young fit males under *RefWind* and *HiWind* conditions, respectively. The number of experiments in each series varied inter-individually and depending on wind condition between 16 and 25 experiments, with total numbers of 97 trials for *RefWind* and 101 for *HiWind*. The average personal characteristics (mean ± SD) of the five participants were 20.1 ± 0.9 years of age, 1.87 ± 0.02 m of body height, 70.5 ± 2.1 kg of body weight, 1.94 ± 0.02 m² of body surface area, and 47.9 ± 6.4 mL/min/kg of maximal oxygen consumption. Before exposure, the participants had undergone a heat acclimation protocol enduring at least three weeks [45].

We briefly summarize the procedures as detailed descriptions are available elsewhere [24]. Each trial consisted of treadmill work with constant workload of walking 4 km/h on the level, which corresponded to the activity level of 2.3 MET, as assumed for *UTCI* [39]. Each trial lasted for at least three hours and consisted of 30 min work periods interrupted by 3 min breaks for determining body weight loss, from which sweat rate (*SR*) was calculated correcting for *ad libitum* fluid ingestion. Under both *HiWind* and *RefWind*, the participants were exposed to varying levels of heat stress with conditions characterized by different combinations of air temperature (T_a; range 25 – 55 °C) and humidity, expressed as water vapour pressure (p_a; 0.5 – 5.3 kPa). Mean radiant temperature (T_{mrt}) was equal to T_a. Trials were stopped prematurely if rectal temperature exceeded 38.5 °C or on the participant's demand.

Rectal temperatures (T_{re}) were recorded continuously using a thermistor probe (YSI 401, YSI Inc., Yellow Springs, Ohio) inserted 10 cm past the anal sphincter. Local skin temperatures were measured with thermistors (YSI 427, YSI Inc., Yellow Springs, Ohio) at the forehead ($T_{sk,head}$), chest ($T_{sk,chest}$), back ($T_{sk,back}$), upper arm ($T_{sk,arm}$), thigh ($T_{sk,thigh}$), and lower leg ($T_{sk,leg}$), and used to calculate mean skin temperature (T_{sk}) as weighted average of the local skin temperatures according to [24], shown in Eq. 3:

$$T_{sk} = 0.05\times T_{sk,head} + 0.2\times T_{sk,chest} + 0.15\times T_{sk,back} + 0.2\times T_{sk,arm} + 0.25\times T_{sk,thigh} + 0.15\times T_{sk,leg} \quad (3)$$

Heart rates (*HR*) were obtained using ECG electrodes, and stored in one-minute intervals, as were T_{re} and T_{sk}. As illustrated by the yellow shaded areas in Figure 1, the averages of T_{re}, *HR*, T_{sk}, and *SR* over the third hour of exposure representing steady-state [25] were submitted to the following data analysis.

2.2. Data analysis and statistics

Penalized regression splines fitted by generalized additive models (GAM) provide a flexible modelling framework for irregularly distributed data [46] allowing for non-linear [47] and random effects [48].

$$E[Y_{ij}] = \mu + s(ID_i) + te(T_{a,ij}, p_{a,ij}) + te_{\Delta v}(T_{a,ij}, p_{a,ij}) + \varepsilon_{ij} \quad (4)$$

Using the notation from Eq. 4 [46], we predicted *HR*, T_{re}, T_{sk}, and *SR*, respectively, as responses from experiment *j* of participant *i* (Y_{ij}) by separate GAMs. These models included an overall intercept

Preprints (www.preprints.org) | NOT PEER-REVIEWED | Posted: 3 May 2023 doi:10.20944/preprints202305.0152.v1

μ, and a bivariate penalized tensor regression spline $te(T_{a,ij}, p_{a,ij})$ for the effects of air temperature and humidity depending on the (T_a, p_a)-combinations, accounting for the repeated measurements by subject-specific intercepts as random coefficients $s(ID_i)$ [48]. Adding another bivariate spline $te_{\Delta v}(T_{a,ij}, p_{a,ij})$ as so called factor smooth interaction [46] of the regression splines with the wind condition (*RefWind* vs *HiWind*), we obtained estimates for the wind effect Δ_v, i.e. the response difference under *HiWind* compared to *RefWind* over the (T_a, p_a) grid supplemented by *p*-values [49]. These were then visualized in a difference plot [50].

More specifically, $s(ID_i)$ refers to a cubic regression spline with basis dimension (or rank) set to k=5 (i.e. with k–1=4 as upper limit of the associated degrees of freedom). Similarly, $te(T_{a,ij}, p_{a,ij})$ and $te_{\Delta v}(T_{a,ij}, p_{a,ij})$ represent tensor products of two cubic regression spline bases for the T_a and p_a dimension, respectively, each of rank k=9, and are hence of total rank k=81. Maximum likelihood parameter estimates with standard errors and *p*-values were obtained assuming Gaussian error ϵ_{ij} [49]. Calculations were performed with the R software version 4.2.1 [51] using the package *mgcv* [46] together with *mgcViz* [50] and *tidymv* [52].

2.3. UTCI calculations

We calculated *UTCI* values using the regression polynomial as described in the *UTCI* operational procedure [39] for given combinations of air temperature (T_a), ambient water vapour pressure (p_a), air velocity 10 m above ground ($v_{a,10m}$), and mean radiant temperature (T_{mrt}). Then, we computed the effect of actual wind speed $v_{a,10m}$ on *UTCI* ($\Delta_v UTCI$) compared to the reference wind speed ($v_{a,10m,ref}$ = 0.5 m/s), while keeping the other parameters constant, as shown in Eq. 5:

$$\Delta_v UTCI = UTCI(T_a;p_a;v_{a,10m};T_{mrt}) - UTCI(T_a;p_a;v_{a,10m,ref};T_{mrt}) \quad (5)$$

Matching the range of experimental climatic conditions (section 2.1), but respecting the upper limits of *UTCI* validity [39,53], we computed *UTCI* and $\Delta_v UTCI$ for combinations of T_a between 25 – 50 °C and of p_a from 0.1 – 5 kPa with relative humidity $rH \leq 100\%$, while setting $T_{mrt} = T_a$ as in the experiments. We performed the calculations for the reference wind speed ($v_{a,10m,ref}$ = 0.5 m/s) matching *RefWind* with $v_{a,1m}$ = 0.3 m/s (Figure 2) and increased wind speeds with $v_{a,10m}$ = 3 m/s matching *HiWind* with $v_{a,1m}$ = 2 m/s.

Supplemental calculations were performed for assessing the modifying effect of radiant heat load by increasing $\Delta T_{mrt}=T_{mrt}-T_a$ from 0 to 30 K in steps of 10 K. In addition, we considered conditions with higher wind speeds $v_{a,10m}$ = 4 and 6 m/s, respectively. Here, $v_{a,10m}$ = 4 m/s corresponds to an increase of 1.7 m/s in relative air velocity at body level ($v_{ar,1m}$) according to Figure 2, matching the settings of the climate chamber experiments; whereas $v_{a,10m}$ = 6 m/s ($v_{a,1m}$ = 4 m/s) parallels the wind speed applied in several simulations and experimental studies [15,17–20,28].

3. Results

Section 3.1 presents the wind effects (*HiWind* vs *RefWind*) evaluated by *UTCI*, and section 3.2 contains the corresponding analyses for the experimental heat strain data, while section 3.3 relates the physiological wind effects to the *UTCI* assessment. Eventually, section 3.4 shows the results for the supplemental *UTCI* analyses considering higher wind speeds and the influence of thermal radiation.

3.1. Wind effects assessed by UTCI

The psychrometric charts in Figure 3 display *UTCI* contours for selected index values representing the upper limits of the *UTCI* heat stress categories in relation to air temperature and humidity for the different wind speeds (Figure 3a). The contours were bended upwards to the left indicating that heat stress increased with temperature and humidity, as expected [36,39]. The dashed lines (*HiWind*) were above the solid lines (*RefWind*) indicating wind cooling at temperatures below 34–35 °C and for hot-humid conditions. On the other hand, dashed lines below solid lines indicating heating by wind were found for hot-dry conditions. The dot-dashed line connecting the intersections of the *RefWind* and *HiWind* contours represents zero wind effect $\Delta_v UTCI$ = 0.

Preprints (www.preprints.org) | NOT PEER-REVIEWED | Posted: 3 May 2023 doi:10.20944/preprints202305.0152.v1

Figure 3b quantifies the magnitude of the wind effect $\Delta_v UTCI$ depending on temperature and humidity. Wind cooling (blueish) increased with decreasing temperature and increasing humidity while heating due to wind (reddish) increased with increasing temperature and decreasing humidity.

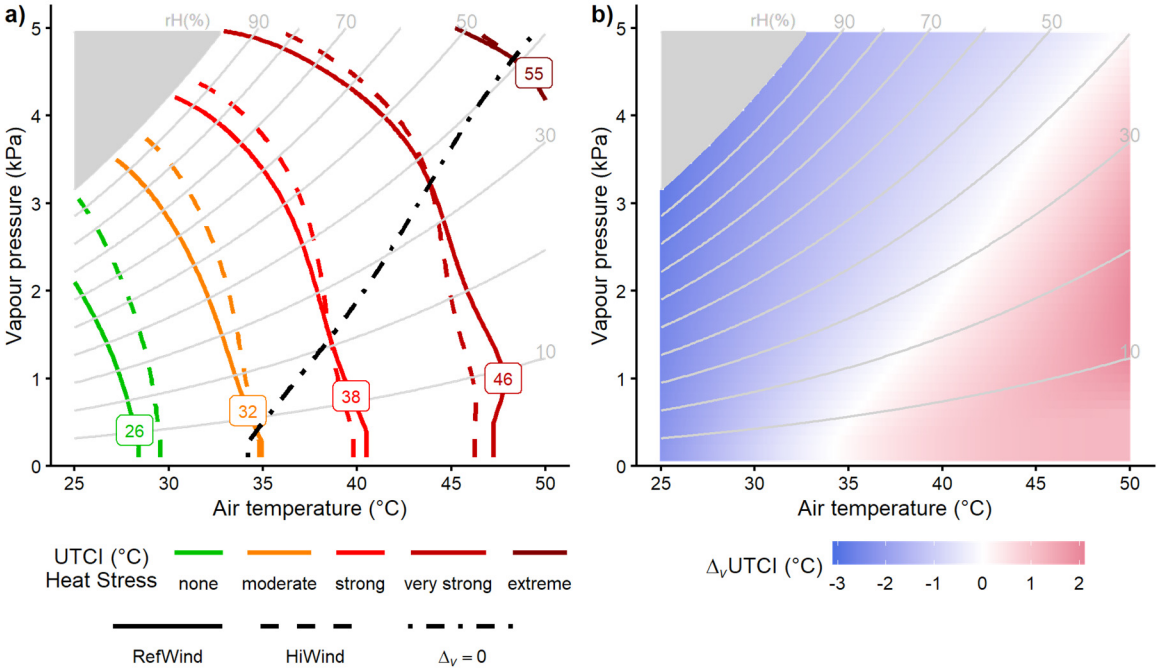

Figure 3. Psychrometric charts showing (**a**) *UTCI* contours related to air temperature and humidity (vapour pressure) representing the upper limits of 'no thermal stress' (*UTCI* = 26 °C), and 'moderate' (32 °C), 'strong' (38 °C), 'very strong' (46 °C) heat stress, as well as an illustrative value for 'extreme heat stress' (55 °C), respectively. The influence of increased wind speed (*HiWind* with $v_{a,10m}$=3 m/s, corresponding to $v_{a,1m}$=2 m/s: dashed lines) is compared to the reference *RefWind* ($v_{a,10m}$=0.5 m/s, corresponding to $v_{a,1m}$=0.3 m/s: solid lines). The dot-dashed line connecting the intersections of *RefWind* with *HiWind* contours represent zero wind effects (Δ_v=0). This line is redrawn in (**b**) as white contour together with the coloured regions indicating temperature-humidity combinations with cooling (blueish) or heating (reddish) wind effects on *UTCI* ($\Delta_v UTCI$) according to Eq. (5), respectively, where colour intensity indicates magnitude. Grey contours mark relative humidity (*rH*) levels. All values were calculated without additional radiant heat load ($\Delta T_{mrt}=T_{mrt}-T_a$=0 K).

3.2. Wind effects on physiological heat strain

Table 1 summarizes the results of the GAMs fitted separately to the physiological heat strain variables. While data for T_{re} were complete, there were a few missing values for *HR*, T_{sk} and *SR*. The estimated mean values of 103 bpm (*HR*), 37.6 °C (T_{re}), 35.5 °C (T_{sk}), and 744 g/h (*SR*), respectively, deemed typical for light to moderate activities under heat stress [24,38]. Goodness-of-fit was good to excellent with more than three quarters of variance explained (R^2>75%) and small residual standard errors for *HR*, T_{re} and T_{sk}. *SR* showed almost 90% explained variance, but a slightly increased standard error, which, however, was still below 125 g/h, considered as the relevant accuracy limit acceptable in occupational or military settings [54]. Moreover, graphical model checking as displayed in the Appendix A by Figure A2 did not reveal any problematic issues concerning the underlying model assumptions.

For all heat strain variables, the splines $te(T_a, p_a)$ modelling the influence of temperature and humidity were statistically highly significant (p<.0001). Similarly, the moderating effects of wind speed as considered by the bivariate interaction splines $te_{\Delta v}(T_a, p_a)$ were statistically significant for *HR*, T_{re}, T_{sk} and *SR*.

Inter-individual variability, as indicated by the random term *s(ID)* played a considerable role (p<.0001) for T_{re}, T_{sk} and *SR*, respectively, whereas individual influences on *HR* appeared to be less pronounced (p = .20).

Preprints (www.preprints.org) | NOT PEER-REVIEWED | Posted: 3 May 2023 doi:10.20944/preprints202305.0152.v1

Table 1. Fitted generalized additive models (GAM) predicting experimental data on heart rate (*HR*), rectal temperature (T_{re}), skin temperature (T_{sk}), and sweat rate (*SR*), respectively, depending on combinations of air temperature (T_a) and vapour pressure (p_a) considering wind condition (*RefWind*, *HiWind*) as modifier and including a random subject effect. Abbreviations for model parameters as in Eq. (4).

	HR (bpm)	***T_{re} (°C)***	***T_{sk} (°C)***	***SR (g/h)***
Observations (#missing values)	189 (9)	198 (0)	189 (9)	186 (13)
Goodness-of-fit				
Adjusted R^2 (%)	78.8	76.2	88.6	89.9
Residual standard error	7.6	0.2	0.4	120.1
Intercept μ				
Mean estimate	102.5	37.6	35.5	744.4
SE	0.8	0.1	0.2	27.1
p-value	<.0001	<.0001	<.0001	<.0001
s(ID)				
edf	0.5	3.8	3.8	3.4
Ref.df	4.0	4.0	4.0	4.0
F-value	0.2	27.1	24.3	6.1
p-value	0.2018	<.0001	<.0001	<.0001
te(T_a, p_a)				
edf	14.6	6.5	10.3	10.0
Ref.df	19.0	8.2	14.0	13.4
F-value	18.9	34.7	31.5	51.3
p-value	<.0001	<.0001	<.0001	<.0001
te$_{\Delta v}$(T_a, p_a)				
edf	4.0	4.0	5.5	4.5
Ref.df	4.1	4.0	6.2	4.8
F-value	10.8	7.0	4.8	8.3
p-value	<.0001	<.0001	0.0001	<.0001

Notes: SE: standard error; edf: effective degrees-of-freedom; Ref.df: reference degrees-of-freedom [55]; s*(ID)*: random subject effect spline; *te(T_a, p_a)*: temperature-humidity effect (bivariate tensor product spline); *te$_{\Delta v}$(T_a, p_a)*: temperature-humidity depending wind effect of *HiWind* compared to *RefWind* (bivariate interaction spline).

Analogous to the *UTCI* results from Figure 3a, Figure 4 displays the effect of temperature and humidity separately for *RefWind* and *HiWind* as contours for the physiological heat strain responses of *HR*, T_{re}, T_{sk} and *SR*. Although the shape of the lines varied between the four variables, and additionally depended on the strain level, a general pattern emerged with contours bended upwards to the left indicating strain levels increasing with temperature and humidity, as it had also occurred for *UTCI* (Figure 3a). Again similar to *UTCI*, the dashed lines (*HiWind*) were above the solid lines (*RefWind*) at low temperatures and under hot-humid conditions demonstrating reduced strain due to wind cooling, whereas for hot-dry climates, the opposite was found with solid lines above dashed lines indicating higher strain levels with increased wind speed.

Preprints (www.preprints.org) | NOT PEER-REVIEWED | Posted: 3 May 2023 doi:10.20944/preprints202305.0152.v1

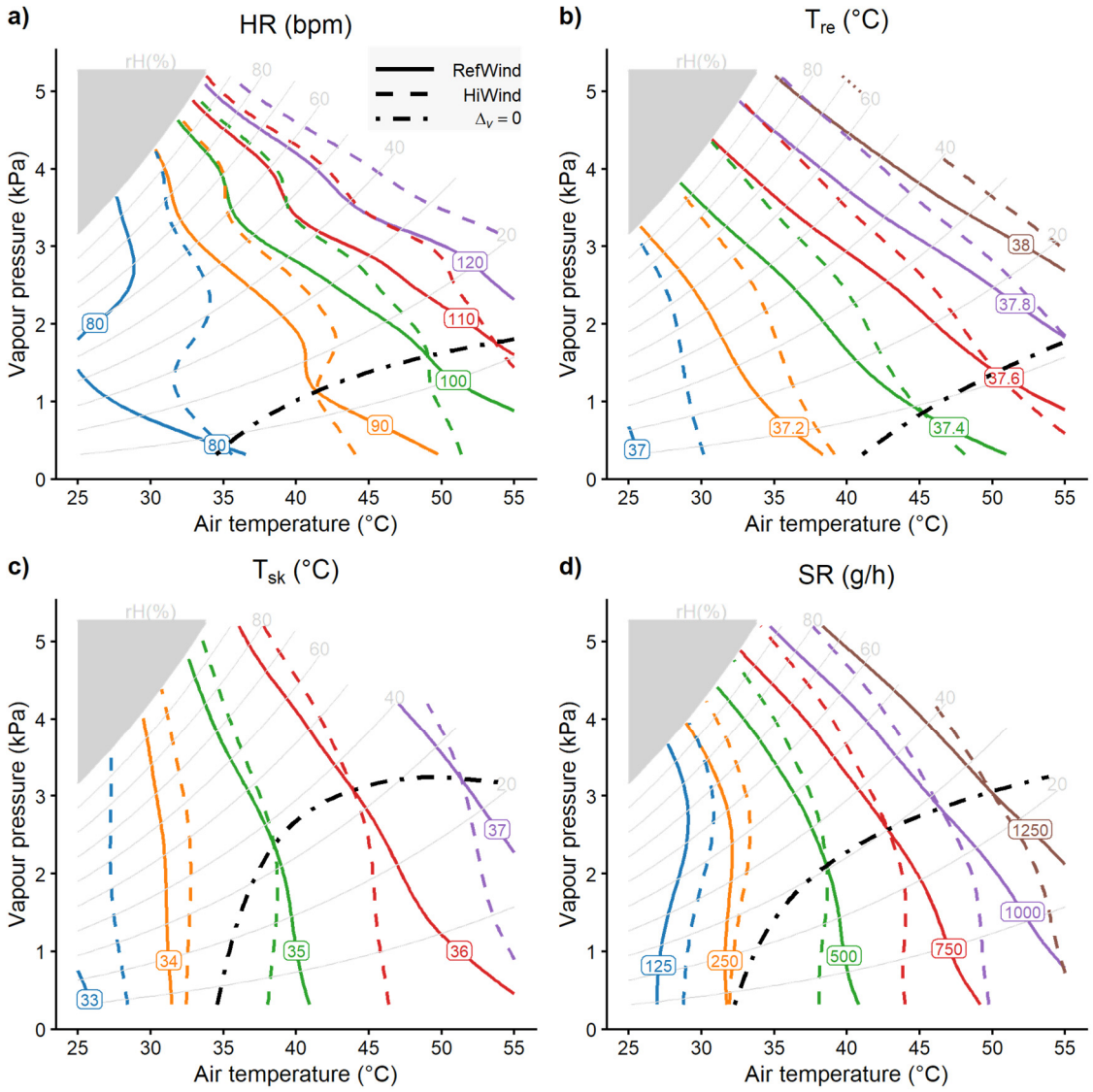

Figure 4. Psychrometric charts including contours of predicted values fitted by GAM to (**a**) heart rates (*HR*), (**b**) rectal temperatures (T_{re}), (**c**) mean skin temperatures (T_{sk}), and (**d**) sweat rates (*SR*) in relation to air temperature and vapour pressure under *RefWind* (solid lines) and *HiWind* conditions (dashed lines), respectively. Dot-dashed lines connecting the intersections of *RefWind* with *HiWind* contours indicate zero wind effects (Δ_v=0).

The dot-dashed lines representing zero wind effect $\Delta_v = 0$, thus marking the threshold separating cooling from heating effects, was bended upwards right similar as for *UTCI* (Figure 3b), but with a greater curvature. They indicated reduced heat strain with *HiWind* at low temperatures and for hot-humid conditions, with limiting vapour pressure above 2 kPa for *HR* and T_{re}, and above 3 kPa for T_{sk} and *SR*, respectively.

The difference plots in Figure 5 show the intensity of the cooling (blueish) and heating (reddish) wind effects over the temperature-humidity grid estimated by GAM, where white areas indicate indifferent temperature-humidity combinations with statistically non-significant differences from $\Delta_v = 0$.

Whereas no significant core temperature increase due to wind was observed, detrimental wind effects with increased *HR*, T_{sk} and *SR* were found under hot-arid conditions with temperature above 40 °C and vapour pressure below 1 kPa. Temperatures below 35 °C yielded no detrimental wind effects.

Preprints (www.preprints.org) | NOT PEER-REVIEWED | Posted: 3 May 2023 doi:10.20944/preprints202305.0152.v1

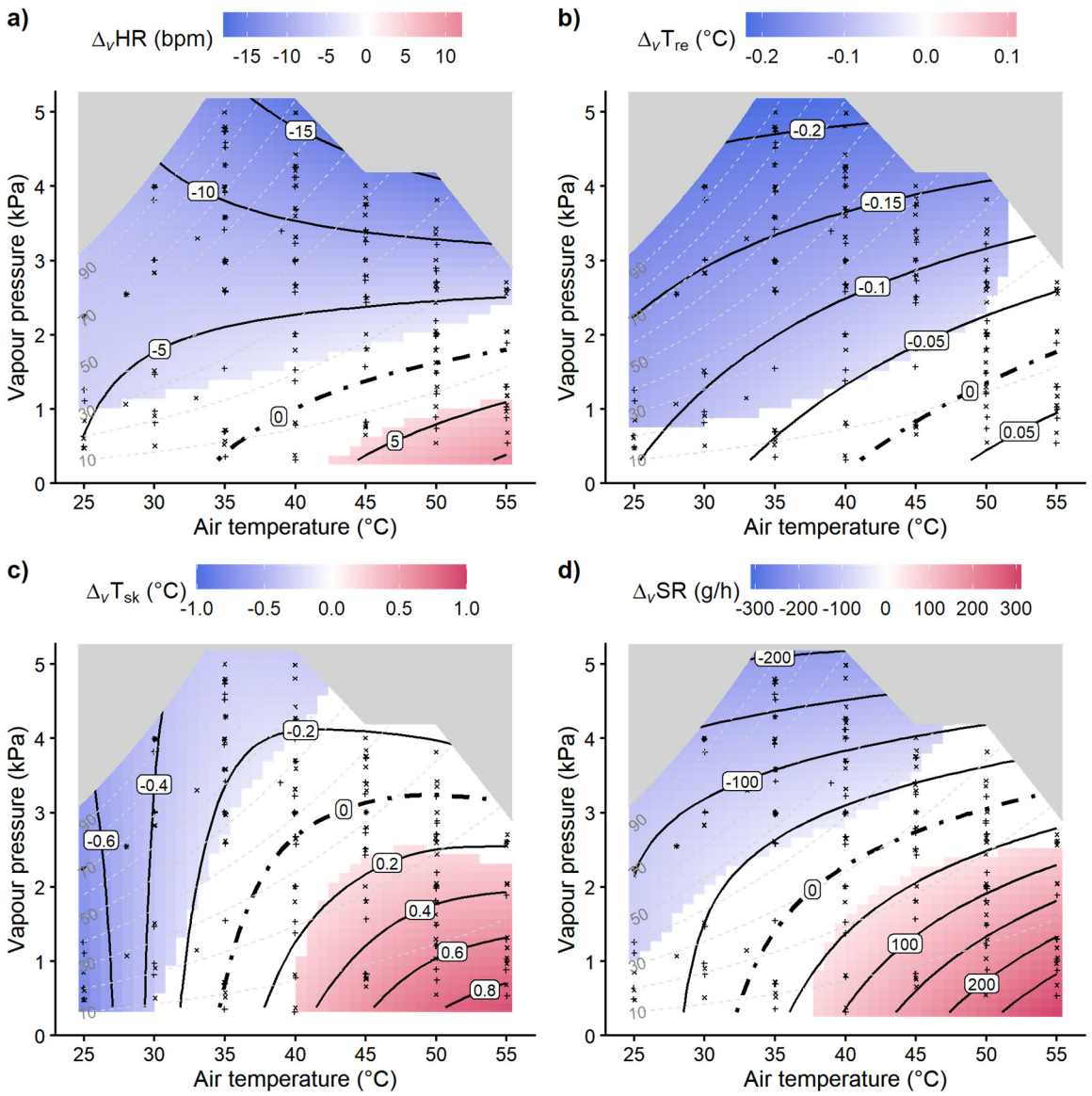

Figure 5. Difference plots with contours of the wind effects (Δv) estimated by GAM in relation to air temperature and vapour pressure for (**a**) heart rates (*HR*), (**b**) rectal temperatures (T_{re}), (**c**) mean skin temperatures (T_{sk}), and (**d**) sweat rates (*SR*). White areas indicate temperature-humidity regions with non-significant wind effects (p>.05 testing for Δ_v=0 vs Δ_v≠0), the blueish areas mark significant reductions in physiological strain by wind cooling, while reddish areas depict significantly increased strain levels due to heating wind effects, respectively. Dashed lines show relative humidity levels; and the grey shaded areas indicate combinations not supported by data. Experimental conditions are marked by '+' (*RefWind*) and '×' (*HiWind*), respectively.

Though significant decreases of core temperature and heart rates by wind under high temperatures started at vapour pressure above 2 kPa, pronounced effects with reductions by more than 10 bpm *HR* or 0.15 °C T_{re} only appeared for very humid conditions with vapour pressure approaching 4 kPa.

3.3. UTCI assessment related to physiological wind effects

The scatterplots in Figure 6 comparing the wind effects (Δ_v) on *UTCI* with the physiological effects showed positive correlations with the closest agreement (r≈0.9) for skin temperature and sweat rate, also concerning the transition from cooling (Δ_v<0) to heating (Δ_v>0) effects. Slightly lower correlations were observed with the effects on heart rates and core temperature.

Preprints (www.preprints.org) | NOT PEER-REVIEWED | Posted: 3 May 2023 doi:10.20944/preprints202305.0152.v1

In addition to correlation analyses, the plots give an indication for the capacity of *UTCI* for correctly classifying conditions with physiological wind cooling or heating [56]. The dashed reference lines in Figure 6 divide the plot in quadrants with the lower left quadrant showing the physiological cooling events correctly assessed by *UTCI* and the upper right containing the correctly assessed heating events, which dominate concerning T_{sk} and *SR*.

Whereas hardly any data points were present in the upper left quadrant with wind cooling falsely predicted by *UTCI*, the conditions collected in the lower right quadrants (falsely predicted heating) concur with a more conservative *UTCI* assessment of the transition from cooling to heating wind concerning *HR* and T_{re}.

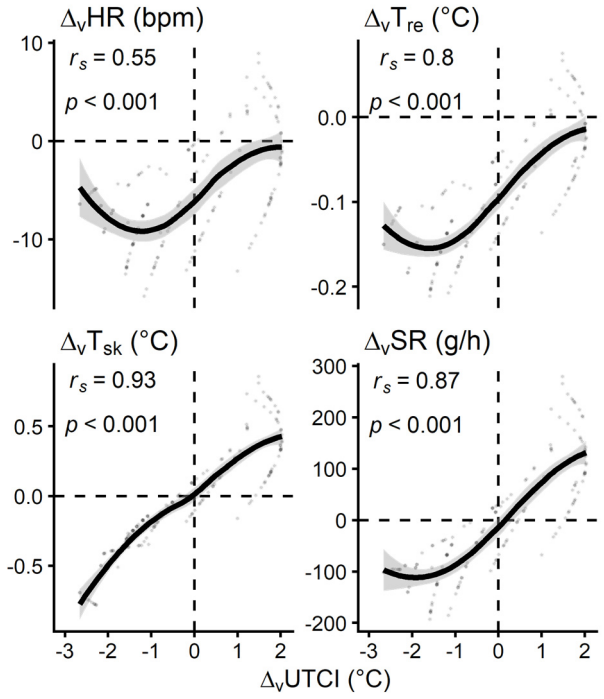

Figure 6. Correlation of wind effects from Figure 5 for heart rate ($\Delta_v HR$), rectal temperature ($\Delta_v T_{re}$), mean skin temperature ($\Delta_v T_{sk}$) and sweat rate ($\Delta_v SR$), respectively, with the wind effect on *UTCI* ($\Delta_v UTCI$) shown in Figure 3b, calculated for the temperature-humidity combinations of the experiments (cf. Figure 5). Spearman correlations (r_s) and *p*-values are shown with smoothing splines and 95%-confidence bands. Dashed vertical and horizontal lines indicate zero wind effects (Δ_v=0) for *UTCI* and the physiological responses, respectively, where negative values (Δ_v<0) indicate wind cooling and positive values (Δ_v>0) heating effects.

3.4. UTCI assessment with higher wind speeds and thermal radiation

Figure A3 in Appendix A visualizes the wind effects (Δ_v) on *UTCI* over the temperature-humidity grid for the different wind speeds and radiant heat loads, expressed as $\Delta T_{mrt} = T_{mrt} - T_a$, with the upper left panel with $v_{a,10m} = 3$ m/s and $\Delta T_{mrt} = 0$ K repeating the data from Figure 3b. Figure 7 summarizes the wind effects $\Delta_v UTCI$ depending on wind speed and radiant heat load as boxplots calculated over the temperature-humidity grid.

As expected, increasing wind speed amplified both the cooling ($\Delta_v UTCI$<0) and heating effects ($\Delta_v UTCI$>0) at the extremes, as indicated by the minima and maxima, but also the 1st and 3rd quartiles in Figure 7. In addition, the threshold line for $\Delta_v UTCI = 0$ slightly shifted towards higher temperatures for higher wind speeds (Figure A3), thus contributing to the decreasing trend with wind speed observed for the median effect in Figure 7.

Concerning the influence of heat radiation on $\Delta_v UTCI$, all percentiles showed a decreasing trend with increasing radiant heat load ΔT_{mrt} (Figure 7). The reduced reddish surface areas with increased radiant heat load in Figure A3 suggest that this was attributable to a massive shift of the threshold

Preprints (www.preprints.org) | NOT PEER-REVIEWED | Posted: 3 May 2023 doi:10.20944/preprints202305.0152.v1

line towards higher temperatures. Thus, wind-cooling effects occurred for a higher portion of climatic conditions over the temperature-humidity grid, shifting the $\Delta_v UTCI$ distribution towards more negative values (Figure 7).

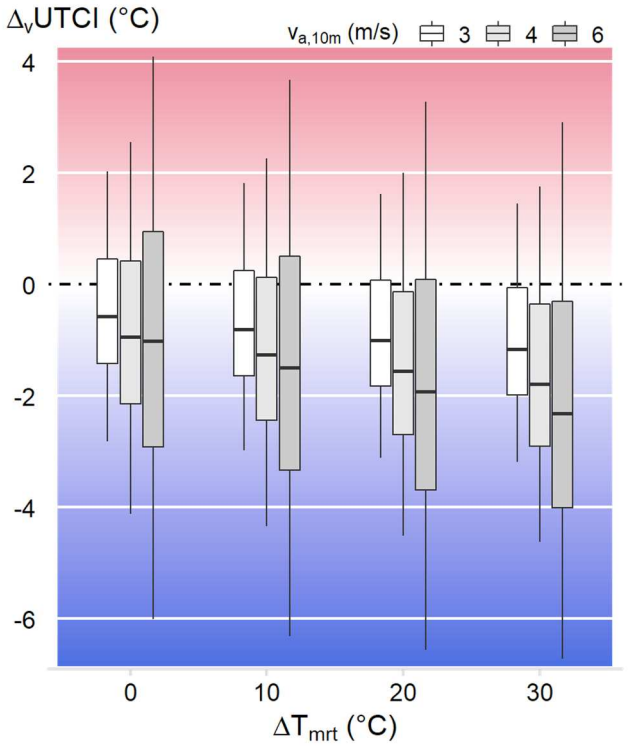

Figure 7. Boxplots including the percentiles P0 (minimum), P25 (1st quartile), P50 (median), P75 (3rd quartile), and P100 (maximum) summarizing the effect of three levels of increased wind speed ($v_{a,10m}$) on *UTCI* ($\Delta_v UTCI$) over air temperatures between 25–50 °C and vapour pressure of 0.1–5 kPa in relation to radiant heat load ($\Delta T_{mrt}=T_{mrt}-T_a$), cf. Figure A3.

The wind effect $\Delta_v UTCI$ at $v_{a,10m}$ = 4 m/s (with ΔT_{mrt} = 0 K) corresponded to the effect of increasing relative air velocity ($v_{ar,1m}$) by 1.7 m/s (Figure 2), conforming to the change in (relative) air velocity realized in the experiments. As the relevant *UTCI* calculations of convective and evaporative heat losses depend on relative air velocity [33], we repeated the correlational analyses from Figure 6 for this condition, as shown in Figure A4. The outcome was very similar as before in Figure 6, though we observed slightly lowered correlations of the physiological wind effects with $\Delta_v UTCI$.

4. Discussion

4.1. Temperature-humdity depending wind effect thresholds

With a view on sustainable heat stress mitigation for moderate activity levels occurring during domestic or industrial work, we assessed the wind effects on physiological heat strain parameters connected with the use of, e.g. electric fans or ventilators. Linking a comprehensive database originating from climate chamber experiments [24] with flexible spline regression models [46], we quantified the physiological heat strain responses of moderately exercising individuals to increasing wind speed over a wide grid of temperature-humidity combinations. Thus, we could derive the temperature-humidity dependent thresholds marking the transition from cooling (Δ_v<0) to heating (Δ_v>0) wind effects on physiological heat strain based on experimental data. This is a distinguishing feature and particular strength of our study, because corresponding experiments with sedentary participants were limited to a few selected climatic conditions [15,16], so that mapping wind effect thresholds in relation to air temperature and humidity for low-active persons had to rely on simulation studies [17–20]. Recently, a study with exercising participants [28] aimed at the interaction

Preprints (www.preprints.org) | NOT PEER-REVIEWED | Posted: 3 May 2023 doi:10.20944/preprints202305.0152.v1

of wind with combinations of temperature and humidity over a likewise extensive grid, but focused on the physical work capacity with cardiac strain clamped at 130 bpm *HR*.

Our experimental findings suggest beneficial, i.e. strain reducing wind effects for temperatures below 35 °C, conforming to common public health recommendations [8–10]. However, beneficial wind effects were also observed at higher temperatures with humidity levels above 2 kPa water vapour pressure concerning heart rate and core temperature, and 3 kPa concerning skin temperature and sweat rate, respectively (Figure 5). This agreed qualitatively with corresponding charts produced in previous studies [19,28]; though there were discrepancies concerning the humidity level separating beneficial wind cooling from detrimental heating effects, which was specified at 50% relative humidity in the former studies, while our study suggested thresholds in terms of absolute humidity (vapour pressure). Some of these discrepancies may be explainable by the 3-h exposures in our study, whereas shorter exposures (1 h) had been used in previous studies [28], with longer exposure times usually resulting in higher strain levels [25,57]. The lower humidity limits for skin temperature and sweat rates compared to core temperature and heart rates in our study may reflect the direct influence of wind speed on the heat transfer from the skin surface by convection and evaporation, and on sweating efficiency [11–13,58].

For *UTCI*, no limiting humidity in terms of vapour pressure were identified, but wind-cooling effects were evident for any temperature condition with relative humidity above 50% (Figure 3b). *UTCI* assessment of wind effects showed high positive correlations with the observed changes in physiological responses (Figure 6), exhibiting the closest agreement (r=0.9) for skin temperature and sweat rate, where wind is known for elevating the relevant convective and evaporative heat transfer as discussed before. *UTCI* showed also a good agreement concerning the transition from cooling (Δ_v<0) to heating (Δ_v>0) wind effects on skin temperatures and sweat rates. The *UTCI* assessment was more conservative, i.e. overpredictive concerning the potentially hazards due to additional heating by wind with respect to core temperature and heart rates (Figure 6).

The expanded *UTCI* calculations suggested that further increasing wind speed would amplify the cooling and heating effects depending on temperature and humidity (Figure A3, Figure 7). In addition, these calculations pointed to a relevant interaction with radiant heat load, e.g. arising from outdoor exposure to solar radiation. Elevated radiant heat load will increase *UTCI* by approximately 3 °C per 10 K increase in ΔT_{mrt} [36]. On the other hand, the limit for beneficial wind-cooling was shifted towards higher temperatures, counteracting, at least partly the heat gained from increased radiant heat load. Similar interaction effects with wind decreasing the heat gain from radiant heat had been reported from thermal manikin measurements with work clothes [59,60]; however, further supporting experimental studies with human participants concerning the interaction of wind with radiant heat load are required.

4.2. Limitations and outlook

The selected study population with young healthy fit males certainly limits the generalizability of our findings, though recent research suggests only minimal influences of individual factors on the heat stress assessment under moderate activity levels [61], as applied in our study. As another limitation, the responses of semi-nude participants (I_{cl} = 0.1 clo) might differ from the effects with clothed humans, e.g. as assumed by *UTCI* with clothing insulation not falling below I_{cl} = 0.3 clo [34]. On the other hand, the prior studies with sedentary participants [15,16] applied similar minimal clothing settings. In addition, limited differences were found concerning the wind effects on physical work capacity with minimal clothing compared to light and covering clothing [28], and the corresponding temperature-humidity charts in that study were produced for a person wearing I_{cl} = 0.28 clo.

Given these limitations, future experimental and modelling studies should consider the moderating influence of individual factors like age, sex or body constitution, and of solar radiation and/or clothing with relevance, e.g. for desert conditions (*simoom*) [21], but also for (semi-)outdoor workplaces.

 doi:10.20944/preprints202305.0152.v1

5. Conclusions

Widening previous findings with resting persons to moderately exercising individuals, our results confirm the wind cooling effects for air temperatures below 35 °C, and corroborate and quantify the potential wind cooling effects at air temperatures above typical skin temperature values in humid climates.

In addition, our findings suggest that *UTCI* has the capability for adequately assessing the heat stress mitigation by wind depending on temperature and humidity under such conditions. Thus, *UTCI* constitutes an easy-to-use tool that may be helpful for establishing evidence-based policies aiming at sustainable heat mitigation strategies under climate change scenarios.

Author Contributions: Conceptualization, P.B. and B.K.; methodology, P.B.; software, P.B.; validation, P.B. and B.K; formal analysis, P.B.; investigation, B.K..; resources, P.B.; data curation, P.B. and B.K.; writing—original draft preparation, P.B.; writing—review and editing, P.B. and B.K.; visualization, P.B.; supervision, B.K.; project administration, P.B. All authors have read and agreed to the published version of the manuscript.

Funding: This research received no external funding.

Institutional Review Board Statement: Not applicable, since this paper makes use of data from prior studies [24,44], which had been conducted in accordance with the Declaration of Helsinki, and approved by the Institutional Ethics Committee of IfADo.

Informed Consent Statement: All participants of the prior studies [24,44] had provided informed consent.

Data Availability Statement: The data presented in this study are available on request from the corresponding author. The data are not publicly available due to data privacy issues.

Acknowledgments: We like to thank the members of the former Environmental Physiology department at IfADo for skillfully running the experiments.

Conflicts of Interest: The authors declare no conflict of interest.

Appendix A

This appendix contains the following supplemental figures:

A1. An additional example of recordings of physiological heat strain variables depending on temperature, humidity and air velocity;
A2. Goodness-of-fit plots for the GAMs fitted to the physiological heat strain variables;
A3. Influence of radiant heat and wind speed on wind effects assessed by *UTCI* ($\Delta_v UTCI$);
A4. Correlations between the wind effects of the physiological heat strain variables with *UTCI* calculated for $v_{a,10m}$ = 4 m/s.

Preprints (www.preprints.org) | NOT PEER-REVIEWED | Posted: 3 May 2023 doi:10.20944/preprints202305.0152.v1

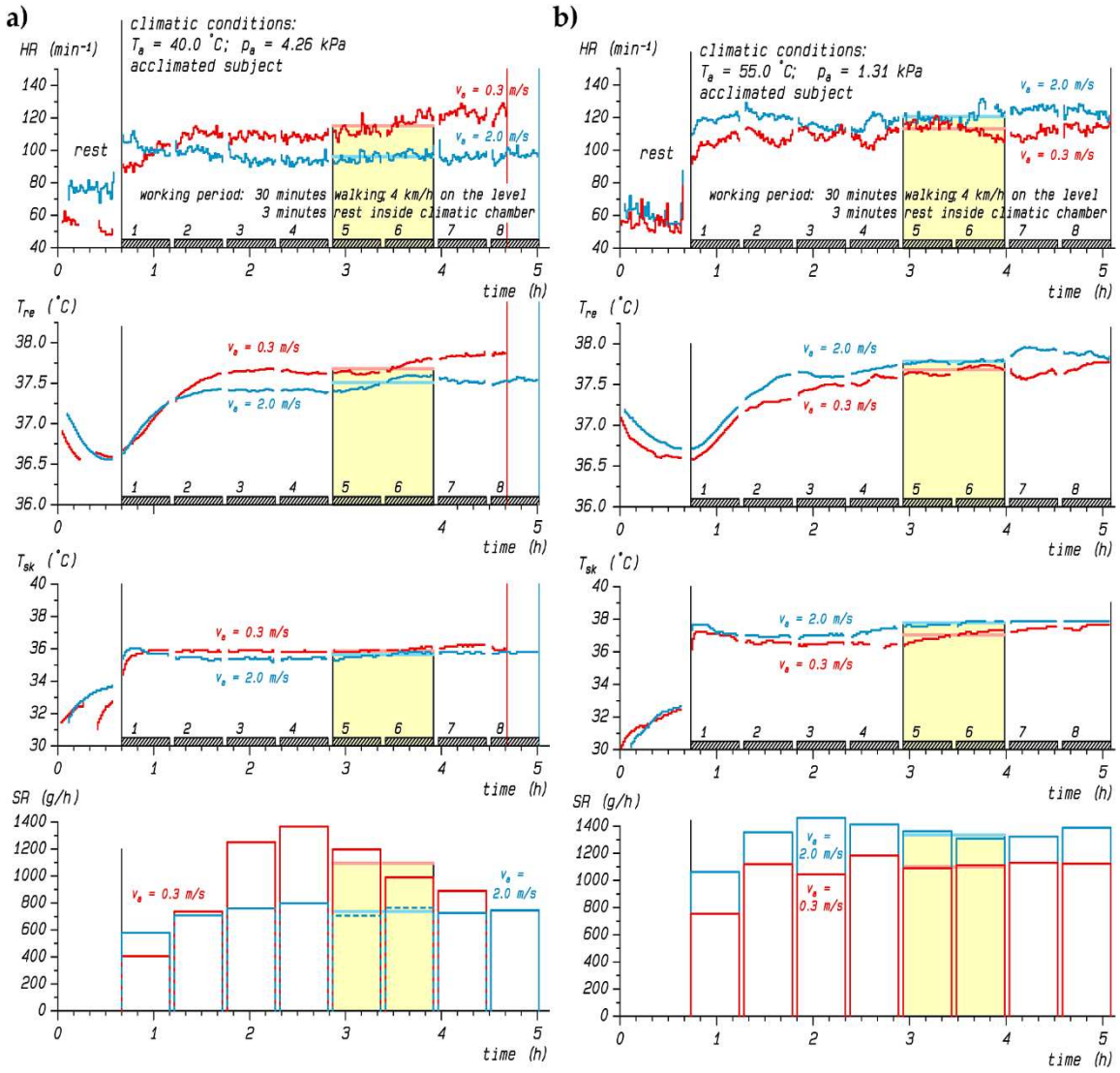

Figure A1. Time course of heart rate (*HR*), rectal (T_{re}) and mean skin temperature (T_{sk}), and sweat rate (*SR*) of an acclimated participant during experiments in a hot-humid climate (**a**) or in a hot-dry climate (**b**) under both a reference (v_a = 0.3 m/s) and a high air velocity (v_a = 2 m/s) condition. The yellow shaded area marks the time interval with averaged values used for analyses. Note that the reference wind trial in (a) was prematurely aborted in the 8th working period.

Preprints (www.preprints.org) | NOT PEER-REVIEWED | Posted: 3 May 2023 doi:10.20944/preprints202305.0152.v1

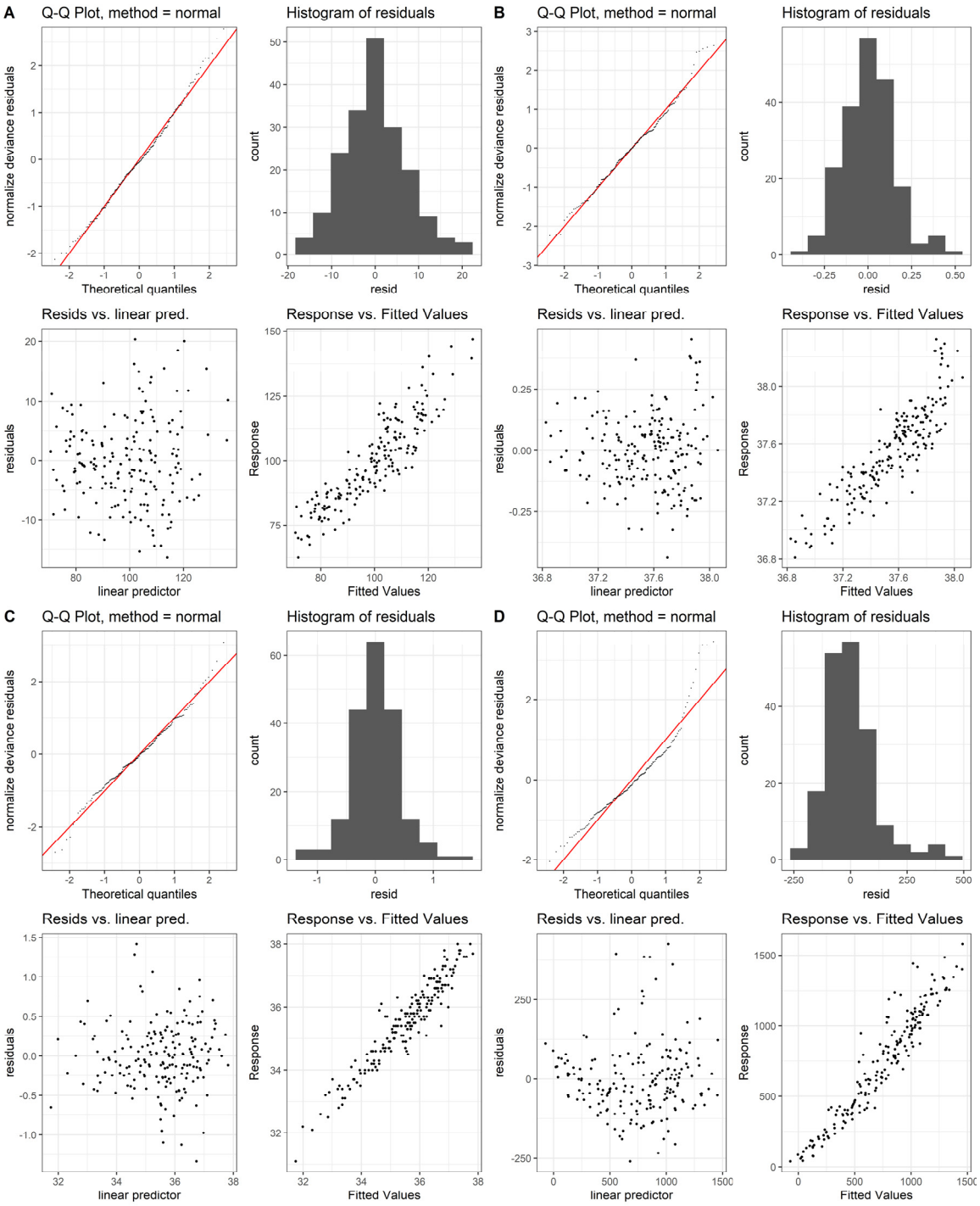

Figure A2. Diagnostic goodness-of-fit plots for the generalized additive models (GAM) fitted to (**A**) heart rate (bpm), (**B**) rectal temperature (°C), (**C**) mean skin temperature (°C), and (**D**) sweat rate (g/h), respectively. The subplots show Q-Q-plots of standardized residuals vs. the theoretical Gaussian quantiles (upper left panels), histograms of residual distribution (upper right), residuals vs. predicted values (lower left), and correlation of observed to fitted values (lower right).

Preprints (www.preprints.org) | NOT PEER-REVIEWED | Posted: 3 May 2023 doi:10.20944/preprints202305.0152.v1

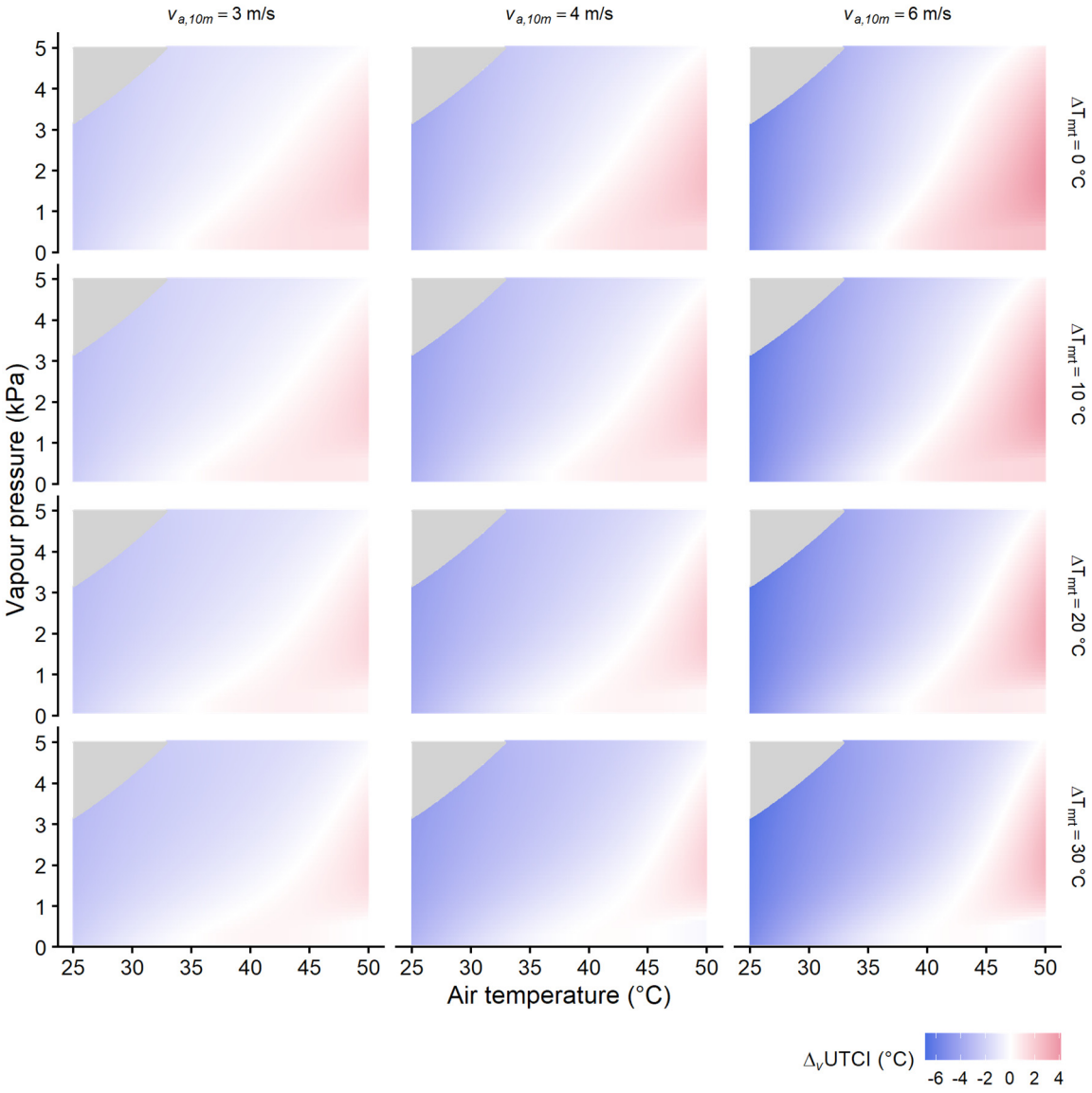

Figure A3. Effect of radiant heat and wind speed on wind effects assessed by *UTCI*. Change in *UTCI* at increased wind speeds ($\Delta_v UTCI$) compared to the reference wind condition ($v_{a,10m}$ = 0.5 m/s) depending on air temperature and vapour pressure considering the influence of radiant heat load ($\Delta T_{mrt}=T_{mrt}-T_a$). Note that the upper left plot replicates the data of Fig. 3b.

Preprints (www.preprints.org) | NOT PEER-REVIEWED | Posted: 3 May 2023 doi:10.20944/preprints202305.0152.v1

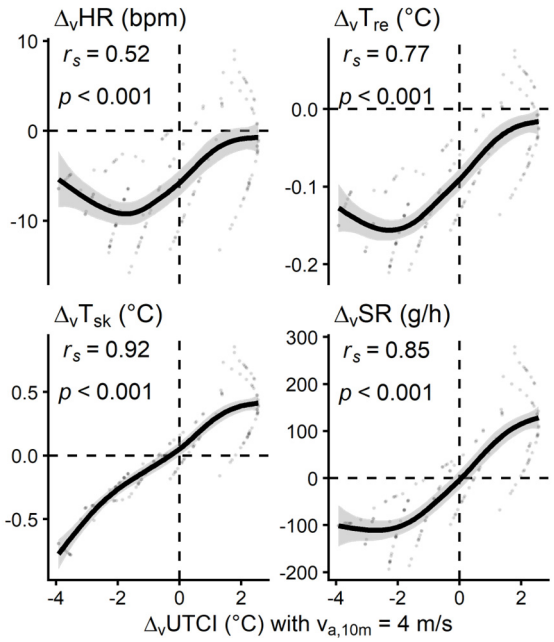

Figure A4. Correlation of wind effects from Figure 5 for heart rate ($\Delta_v HR$), rectal temperature ($\Delta_v T_{re}$), mean skin temperature ($\Delta_v T_{sk}$) and sweat rate ($\Delta_v SR$), respectively, with the wind effect on *UTCI* ($\Delta_v UTCI$) calculated for an elevated wind speed (4 m/s).

References

1. Ebi, K.L.; Capon, A.; Berry, P.; Broderick, C.; de Dear, R.; Havenith, G.; Honda, Y.; Kovats, R.S.; Ma, W.; Malik, A., et al. Hot weather and heat extremes: health risks. *The Lancet* **2021**, *398*, 698-708, doi:10.1016/S0140-6736(21)01208-3.
2. Romanello, M.; Di Napoli, C.; Drummond, P.; Green, C.; Kennard, H.; Lampard, P.; Scamman, D.; Arnell, N.; Ayeb-Karlsson, S.; Ford, L.B., et al. The 2022 report of the Lancet Countdown on health and climate change: health at the mercy of fossil fuels. *The Lancet* **2022**, *400*, 1619-1654, doi:10.1016/S0140-6736(22)01540-9.
3. Foster, J.; Smallcombe, J.W.; Hodder, S.; Jay, O.; Flouris, A.D.; Nybo, L.; Havenith, G. An advanced empirical model for quantifying the impact of heat and climate change on human physical work capacity. *International Journal of Biometeorology* **2021**, *65*, 1215-1229, doi:10.1007/s00484-021-02105-0.
4. Bröde, P.; Fiala, D.; Lemke, B.; Kjellstrom, T. Estimated work ability in warm outdoor environments depends on the chosen heat stress assessment metric. *International Journal of Biometeorology* **2018**, *62*, 331-345, doi:10.1007/s00484-017-1346-9.
5. Jay, O.; Capon, A.; Berry, P.; Broderick, C.; de Dear, R.; Havenith, G.; Honda, Y.; Kovats, R.S.; Ma, W.; Malik, A., et al. Reducing the health effects of hot weather and heat extremes: from personal cooling strategies to green cities. *The Lancet* **2021**, *398*, 709-724, doi:10.1016/S0140-6736(21)01209-5.
6. Malik, A.; Bongers, C.; McBain, B.; Rey-Lescure, O.; Dear, R.d.; Capon, A.; Lenzen, M.; Jay, O. The potential for indoor fans to change air conditioning use while maintaining human thermal comfort during hot weather: an analysis of energy demand and associated greenhouse gas emissions. *The Lancet Planetary Health* **2022**, *6*, e301-e309, doi:10.1016/S2542-5196(22)00042-0.
7. Jay, O.; Hoelzl, R.; Weets, J.; Morris, N.; English, T.; Nybo, L.; Niu, J.; de Dear, R.; Capon, A. Fanning as an alternative to air conditioning – A sustainable solution for reducing indoor occupational heat stress. *Energy and Buildings* **2019**, *193*, 92-98, doi:10.1016/j.enbuild.2019.03.037.
8. CDC. *Frequently Asked Questions (FAQ) About Extreme Heat*; Centers for Disease Control and Prevention: Atlanta, GA, 2020-01-15, 2012. Availabe online: https://www.cdc.gov/disasters/extremeheat/faq.html (accessed on 2020-01-15).
9. EPA. *Excessive Heat Events Guidebook*; EPA 430-B-16-001; United States Environmental Protection Agency: Washington, DC, 2016. Availabe online: https://www.epa.gov/sites/production/files/2016-03/documents/eheguide_final.pdf (accessed on 2020-01-15).
10. McGregor, G.R.; Bessemoulin, P.; Ebi, K.; Menne, B. *Heatwaves and Health: Guidance on Warning-System Development*; WMO-No. 1142; World Meteorological Organization and World Health Organization:

Geneva, 2015. Availabe online: https://library.wmo.int/doc_num.php?explnum_id=3371 (accessed on 2020-01-15).
11. Candas, V.; Libert, J.P.; Vogt, J.J. Influence of air velocity and heat acclimation on human skin wettedness and sweating efficiency. *Journal of Applied Physiology* **1979**, *47*, 1194-1200, doi:10.1152/jappl.1979.47.6.1194.
12. Adams, W.C.; Mack, G.W.; Langhans, G.W.; Nadel, E.R. Effects of varied air velocity on sweating and evaporative rates during exercise. *Journal of Applied Physiology* **1992**, *73*, 2668-2674, doi:10.1152/jappl.1992.73.6.2668.
13. Nadel, E.R.; Stolwijk, J.A. Effect of skin wettedness on sweat gland response. *Journal of Applied Physiology* **1973**, *35*, 689-694, doi:10.1152/jappl.1973.35.5.689.
14. Jay, O.; Capon, A. Use of physiological evidence for heatwave public policy. *The Lancet Planetary Health* **2018**, *2*, e10, doi:10.1016/S2542-5196(17)30178-X.
15. Morris, N.B.; English, T.; Hospers, L.; Capon, A.; Jay, O. The Effects of Electric Fan Use Under Differing Resting Heat Index Conditions: A Clinical Trial. *Annals of Internal Medicine* **2019**, *171*, 675-677, doi:10.7326/m19-0512.
16. Ravanelli, N.M.; Hodder, S.G.; Havenith, G.; Jay, O. Heart Rate and Body Temperature Responses to Extreme Heat and Humidity With and Without Electric Fans. *JAMA* **2015**, *313*, 724-725, doi:10.1001/jama.2015.153.
17. Morris, N.B.; Chaseling, G.K.; English, T.; Gruss, F.; Maideen, M.F.B.; Capon, A.; Jay, O. Electric fan use for cooling during hot weather: a biophysical modelling study. *The Lancet Planetary Health* **2021**, *5*, e368-e377, doi:10.1016/S2542-5196(21)00136-4.
18. Tartarini, F.; Schiavon, S.; Jay, O.; Arens, E.; Huizenga, C. Application of Gagge's energy balance model to determine humidity-dependent temperature thresholds for healthy adults using electric fans during heatwaves. *Building and Environment* **2021**, *207*, 108437, doi:10.1016/j.buildenv.2021.108437.
19. Hospers, L.; Smallcombe, J.W.; Morris, N.B.; Capon, A.; Jay, O. Electric fans: A potential stay-at-home cooling strategy during the COVID-19 pandemic this summer? *Science of The Total Environment* **2020**, *747*, 141180, doi:10.1016/j.scitotenv.2020.141180.
20. Jay, O.; Cramer, M.N.; Ravanelli, N.M.; Hodder, S.G. Should electric fans be used during a heat wave? *Applied Ergonomics* **2015**, *46*, 137-143, doi:10.1016/j.apergo.2014.07.013.
21. Normand, C.W.B. The effect of high temperature, humidity, and wind on the human body. *Quarterly Journal of the Royal Meteorological Society* **1920**, *46*, 1-14, doi:10.1002/qj.49704619302.
22. Ainsworth, B.E.; Haskell, W.L.; Herrmann, S.D.; Meckes, N.; Bassett, D.R.J.; Tudor-Locke, C.; Greer, J.L.; Vezina, J.; Whitt-Glover, M.C.; Leon, A.S. 2011 Compendium of Physical Activities: A Second Update of Codes and MET Values. *Medicine & Science in Sports & Exercise* **2011**, *43*, 1575-1581, doi:10.1249/MSS.0b013e31821ece12.
23. ISO 8996. *Ergonomics of the thermal environment – Determination of metabolic rate*; International Organisation for Standardisation: Geneva, 2021.
24. Kampmann, B. Zur Physiologie der Arbeit in warmem Klima. Ergebnisse aus Laboruntersuchungen und aus Feldstudien im Steinkohlenbergbau. Habilitation Thesis, Bergische Universität Wuppertal, Wuppertal, 2000.
25. Kampmann, B.; Bröde, P. Do one-hour exposures provide a valid assessment of physiological heat strain? *Zeitschrift für Arbeitswissenschaft* **2022**, *76*, 105-117, doi:10.1007/s41449-022-00303-z.
26. Brown, W.K.; Sargent, F. Hidromeiosis. *Archives of Environmental Health: An International Journal* **1965**, *11*, 442-453, doi:10.1080/00039896.1965.10664244.
27. Candas, V.; Libert, J.; Vogt, J. Effect of hidromeiosis on sweat drippage during acclimation to humid heat. *European Journal of Applied Physiology and Occupational Physiology* **1980**, *44*, 123-133, doi:10.1007/BF00421090.
28. Foster, J.; Smallcombe, J.W.; Hodder, S.; Jay, O.; Flouris, A.D.; Havenith, G. Quantifying the impact of heat on human physical work capacity; part II: the observed interaction of air velocity with temperature, humidity, sweat rate, and clothing is not captured by most heat stress indices. *International Journal of Biometeorology* **2021**, *66*, 507-520, doi:10.1007/s00484-021-02212-y.
29. Kamon, E.; Avellini, B. Wind speed limits to work under hot environments for clothed men. *Journal of Applied Physiology* **1979**, *46*, 340-345, doi:10.1152/jappl.1979.46.2.340.
30. Graham, C.; Lynch, G.P.; English, T.; Hospers, L.; Jay, O. Optimal break structures and cooling strategies to mitigate heat stress during a Rugby League match simulation. *Journal of Science and Medicine in Sport* **2021**, *24*, 793-799, doi:10.1016/j.jsams.2021.04.013.
31. Wang, F.; Deng, Q.; Lei, T.-H.; Wang, X.; Wang, A.R. Biophysical modelling predicts unreliable core temperature responses on healthy older adults using electric fans at residential homes during heatwaves. *Building and Environment* **2023**, *228*, 109888, doi:10.1016/j.buildenv.2022.109888.
32. Jendritzky, G.; de Dear, R.; Havenith, G. UTCI - Why another thermal index? *International Journal of Biometeorology* **2012**, *56*, 421-428, doi:10.1007/s00484-011-0513-7.

33. Fiala, D.; Havenith, G.; Bröde, P.; Kampmann, B.; Jendritzky, G. UTCI-Fiala multi-node model of human heat transfer and temperature regulation. *International Journal of Biometeorology* **2012**, *56*, 429-441, doi:10.1007/s00484-011-0424-7.
34. Havenith, G.; Fiala, D.; Blazejczyk, K.; Richards, M.; Bröde, P.; Holmér, I.; Rintamaki, H.; Ben Shabat, Y.; Jendritzky, G. The UTCI-clothing model. *International Journal of Biometeorology* **2012**, *56*, 461-470, doi:10.1007/s00484-011-0451-4.
35. Psikuta, A.; Fiala, D.; Laschewski, G.; Jendritzky, G.; Richards, M.; Blazejczyk, K.; Mekjavic, I.B.; Rintamäki, H.; de Dear, R.; Havenith, G. Validation of the Fiala multi-node thermophysiological model for UTCI application. *International Journal of Biometeorology* **2012**, *56*, 443-460, doi:10.1007/s00484-011-0450-5.
36. Bröde, P.; Blazejczyk, K.; Fiala, D.; Havenith, G.; Holmér, I.; Jendritzky, G.; Kuklane, K.; Kampmann, B. The Universal Thermal Climate Index UTCI Compared to Ergonomics Standards for Assessing the Thermal Environment. *Industrial Health* **2013**, *51*, 16-24, doi:10.2486/indhealth.2012-0098.
37. Kampmann, B.; Bröde, P.; Fiala, D. Physiological responses to temperature and humidity compared to the assessment by UTCI, WGBT and PHS. *International Journal of Biometeorology* **2012**, *56*, 505-513, doi:10.1007/s00484-011-0410-0.
38. Ioannou, L.G.; Tsoutsoubi, L.; Mantzios, K.; Vliora, M.; Nintou, E.; Piil, J.F.; Notley, S.R.; Dinas, P.C.; Gourzoulidis, G.A.; Havenith, G., et al. Indicators to assess physiological heat strain – Part 3: Multi-country field evaluation and consensus recommendations. *Temperature* **2022**, *9*, 274-291, doi:10.1080/23328940.2022.2044739.
39. Bröde, P.; Fiala, D.; Blazejczyk, K.; Holmér, I.; Jendritzky, G.; Kampmann, B.; Tinz, B.; Havenith, G. Deriving the operational procedure for the Universal Thermal Climate Index (UTCI). *International Journal of Biometeorology* **2012**, *56*, 481-494, doi:10.1007/s00484-011-0454-1.
40. Sadeghi, M.; de Dear, R.; Wood, G.; Samali, B. Development of a bioclimatic wind rose tool for assessment of comfort wind resources in Sydney, Australia for 2013 and 2030. *International Journal of Biometeorology* **2018**, *62*, 1963-1972, doi:10.1007/s00484-018-1597-0.
41. Foster, J.; Smallcombe, J.W.; Hodder, S.; Jay, O.; Flouris, A.D.; Nybo, L.; Havenith, G. Quantifying the impact of heat on human physical work capacity; part III: the impact of solar radiation varies with air temperature, humidity, and clothing coverage. *International Journal of Biometeorology* **2022**, *66*, 175-188, doi:10.1007/s00484-021-02205-x.
42. ISO 11079. *Ergonomics of the thermal environment - Determination and interpretation of cold stress when using required clothing insulation (IREQ) and local cooling effects*; International Organisation for Standardisation: Geneva, 2007.
43. ISO 9920. *Ergonomics of the thermal environment - Estimation of thermal insulation and water vapour resistance of a clothing ensemble*; International Organisation for Standardisation: Geneva, 2007.
44. Wenzel, H.G.; Mehnert, C.; Schwarzenau, P. Evaluation of tolerance limits for humans under heat stress and the problems involved. *Scandinavian Journal of Work, Environment & Health* **1989**, *15*, 7-14.
45. Kampmann, B.; Bröde, P. Heat Acclimation Does Not Modify Q10 and Thermal Cardiac Reactivity. *Frontiers in Physiology* **2019**, *10*, 1524, doi:10.3389/fphys.2019.01524.
46. Wood, S.N. *Generalized Additive Models: An Introduction with R*, 2nd ed.; Chapman & Hall/CRC: Boca Raton, Florida, 2017.
47. Zuur, A.F.; Ieno, E.N.; Walker, N.J.; Saveliev, A.A.; Smith, G.M. Things are not Always Linear; Additive Modelling. In *Mixed effects models and extensions in ecology with R*, Zuur, A.F., Ieno, E.N., Walker, N.J., Saveliev, A.A., Smith, G.M., Eds. Springer: New York, 2009; pp. 35-69, doi:10.1007/978-0-387-87458-6_3.
48. Wood, S.N. A simple test for random effects in regression models. *Biometrika* **2013**, *100*, 1005-1010, doi:10.1093/biomet/ast038.
49. Wood, S.N. On p-values for smooth components of an extended generalized additive model. *Biometrika* **2013**, *100*, 221-228, doi:10.1093/biomet/ass048.
50. Fasiolo, M.; Nedellec, R.; Goude, Y.; Wood, S.N. Scalable visualisation methods for modern Generalized Additive Models. *Journal of Computational and Graphical Statistics* **2020**, *29*, 78-86, doi:10.1080/10618600.2019.1629942.
51. R Core Team. R: A Language and Environment for Statistical Computing. R Foundation for Statistical Computing: Vienna, Austria, 2022.
52. Coretta, S. tidymv: Tidy Model Visualisation for Generalised Additive Models. R package version 3.3.1. 2022.
53. Bröde, P. Issues in UTCI Calculation from a Decade's Experience. In *Applications of the Universal Thermal Climate Index UTCI in Biometeorology: Latest Developments and Case Studies*, Krüger, E.L., Ed. Springer International Publishing: Cham, 2021; pp. 13-21, doi:10.1007/978-3-030-76716-7_2.
54. Cheuvront, S.; Montain, S.; Goodman, D.; Blanchard, L.; Sawka, M. Evaluation of the limits to accurate sweat loss prediction during prolonged exercise. *European Journal of Applied Physiology* **2007**, *101*, 215-224, doi:10.1007/s00421-007-0492-x.

55. Wood, S.N. Ref.df in mgcv gam. Availabe online: https://stat.ethz.ch/pipermail/r-help/2019-March/462135.html (accessed on 2023-02-09).
56. Richmond, V.L.; Davey, S.; Griggs, K.; Havenith, G. Prediction of Core Body Temperature from Multiple Variables. *Annals of Occupational Hygiene* **2015**, *59*, 1168-1178, doi:10.1093/annhyg/mev054.
57. Smallcombe, J.W.; Foster, J.; Hodder, S.G.; Jay, O.; Flouris, A.D.; Havenith, G. Quantifying the impact of heat on human physical work capacity; part IV: interactions between work duration and heat stress severity. *International Journal of Biometeorology* **2022**, *66*, 2463-2476, doi:10.1007/s00484-022-02370-7.
58. Nadel, E.R.; Bullard, R.W.; Stolwijk, J.A. Importance of skin temperature in the regulation of sweating. *Journal of Applied Physiology* **1971**, *31*, 80-87, doi:10.1152/jappl.1971.31.1.80.
59. Bröde, P.; Kuklane, K.; Candas, V.; den Hartog, E.A.; Griefahn, B.; Holmér, I.; Meinander, H.; Nocker, W.; Richards, M.; Havenith, G. Heat Gain From Thermal Radiation Through Protective Clothing With Different Insulation, Reflectivity and Vapour Permeability. *International Journal of Occupational Safety and Ergonomics* **2010**, *16*, 231-244.
60. den Hartog, E.A.; Havenith, G. Analytical study of the heat loss attenuation by clothing on thermal manikins under radiative heat loads. *International Journal of Occupational Safety and Ergonomics* **2010**, *16*, 245-261.
61. Wolf, S.T.; Havenith, G.; Kenney, W.L. Relatively minor influence of individual characteristics on critical wet-bulb globe temperature (WBGT) limits during light activity in young adults (PSU HEAT Project). *Journal of Applied Physiology* **2023**, *134*, 1216-1223, doi:10.1152/japplphysiol.00657.2022.